



Published in final edited form as:

Neuroradiology. 2019 April ; 61(4): 431–441. doi:10.1007/s00234-019-02164-6.

Comparison of multi-shot and single shot echo-planar diffusion tensor techniques for the optic pathway in patients with neurofibromatosis type 1

Chang Y. Ho¹, Rachael Deardorff¹, Stephen F. Kralik^{1,2}, John D. West¹, Yu-Chien Wu¹, Chie-Schin Shih³

¹Department of Radiology and Imaging Sciences, Indiana University School of Medicine, Indiana, IN, USA

²Department of Radiology, Texas Children's Hospital, Houston, TX, USA

³Department of Pediatrics, Section of Hematology/Oncology, Indiana University School of Medicine, Indiana, IN, USA

Abstract

Purpose—Diffusion tensor imaging (DTI) may be helpful in assessing optic pathway integrity as a marker for treatment in neurofibromatosis type 1 (NF1) patients with optic gliomas (OG). However, susceptibility artifacts are common in typical single-shot echo planar imaging (ssDTI). A readout-segmented multi-shot EPI technique (rsDTI) was utilized to minimize susceptibility distortions of the skull base and improve quantitative metrics.

Methods—Healthy controls, children with NF1 without OG, and NF1 with OG± visual symptoms were included. All subjects were scanned with both rsDTI and ssDTI sequences sequentially. Diffusion metrics and deterministic fiber tracking were calculated. Tract count, volume, and length were also compared by a two-factor mixed ANOVA.

Results—Five healthy controls, 7 NF1 children without OG, and 12 NF1 children with OG were imaged. Six OG patients had visual symptoms. Four subjects had no detectable optic pathway fibers on ssDTI due to susceptibility, for which rsDTI was able to delineate. Tract count ($p < 0.001$), tract volume ($p < 0.001$), and FA ($P < 0.001$) were significantly higher for rsDTI versus ssDTI for all subjects. MD ($p < 0.001$) and RD ($p < 0.001$) were significantly lower for rsDTI vs ssDTI. Finally, MD, AD, and RD had a significantly lower difference in NF1 children with visual symptoms compared to NF1 children without visual symptoms only on ssDTI scans.

Chang Y. Ho cyho@iupui.edu.

Compliance with ethical standards

Conflict of interest The authors declare that they have no conflict of interest.

Ethical approval All procedures performed in the studies involving human participants were in accordance with the ethical standards of the institutional and/or national research committee and with the 1964 Helsinki Declaration and its later amendments or comparable ethical standards.

Informed consent Informed consent was obtained from all individual participants included in the study.

Publisher's note Springer Nature remains neutral with regard to jurisdictional claims in published maps and institutional affiliations.

Conclusion—DTI with readout-segmented multi-shot EPI technique can better visualize the optic pathway and allow more confident measurements of anisotropy in NF1 patients. This is shown by a significant increase in FA, tract count, and volume with rsDTI versus ssDTI.

Keywords

Neurofibromatosis type 1; Optic nerve glioma; Diffusion tensor imaging

Children with neurofibromatosis type 1 (NF1) have up to a 20% incidence of developing optic pathway glioma (OG) with visual loss affecting up to 50% of these patients with glioma. Visual symptoms include loss of visual acuity, proptosis, strabismus, and nystagmus [1–3]. First-line treatment for OG includes chemotherapy which can improve visual acuity in 32% of treated patients [1]. However, the clinical indication for initiating adjuvant therapy in a patient with an OG detected by imaging is not clear, particularly without detectable visual deficits. Although optic chiasm volume can correlate with visual acuity in other patient populations [4]; within NF1 patients, there is poor correlation of the radiographic size of tumors and visual outcomes [1]. Furthermore, there is difficulty in assessing visual function in very young children who cannot adequately communicate deteriorating visual symptoms or cooperate with visual assessment tests. This is particularly relevant in NF1 patients where the mean age of diagnosis of OG is between 2 and 5 years of age [5,6]. As such, an imaging marker of visual function in NF1 patients may be helpful in determining a threshold point for treatment, as well as to monitor treatment response.

Diffusion tensor imaging (DTI) is an MRI technique which provides a quantitative evaluation of the white matter tracts and may be helpful in assessing optic pathway integrity as an imaging marker for treatment in these patients. However, susceptibility artifacts that are common in typical DTI single-shot echo planar imaging (ssDTI) can severely distort areas of interest such as the optic nerves and optic chiasm, which are immediately adjacent to the air-bone interface from the sinuses and skull base. In addition to susceptibility-induced distortion, the optic nerve is a small structure of less than 3 mm and requires high spatial resolution for proper imaging. One solution to reducing susceptibility artifacts on DTI is to utilize a readout-segmented multi-shot echo-planar-imaging technique (rsDTI), which has shown improved visualization of DWI images in the skullbase particularly for sinonasal lesions [7].

The purpose of this research is to compare diffusion tensor MRI of the optic nerve between ssDTI and rsDTI in healthy volunteers, NF1 patients without OG, and NF1 patients with OG with and without visual symptoms. We hypothesize that rsDTI will be superior to ssDTI both qualitatively and in measured quantitative parameters due to less susceptibility artifact.

Participants and methods

The prospective study was approved by the Indiana University institutional review board. Written informed consent was obtained from patients greater than or equal to 18 years of age or from parents/legal guardians of children less than 18 years, with child assent when appropriate according to institutional policy.

Healthy children (HC) without a history of NF1 or visual symptoms, children with NF1 without OG, and NF1 with OG with and without visual symptoms were recruited. Healthy controls were recruited through advertisements and were screened for past medical history, surgery, or visual symptoms with a patient questionnaire. Patients with prior cancers, chemotherapeutic treatment, and visual symptoms were excluded. NF1 patients were recruited from a pediatric NF1 clinic. Visual symptoms and concurrent chemotherapy treatment history were obtained from an electronic patient database. The existence of an optic pathway tumor was determined by prior MRI results. OG was defined as an enhancing or nonenhancing optic pathway mass that abnormally expanded the optic pathway compared to the contralateral side. All NF1 patients with OG had an ophthalmology referral for visual symptom assessment.

Both rsDTI and ssDTI were obtained sequentially in the same scan session. Diffusion images were acquired on 3 T scanners (Verio and Skyra, Siemens MAGNETOM, Erlangen, Germany) with the following parameters for product ssDTI (Verio/Skyra; TR: 4200/2500 ms, TE: 152/86 ms, Bandwidth: 1085/1210, Echo Spacing: 0.94 ms, Flip Angle:90, matrix:192 × 192/180 × 180, no gap, IPAT = 2) and rsDTI using readout segmentation of long variable echotrails (RESOLVE; Siemens, Erlangen, Germany) (TR:2800/2320 ms, TE:70/68 ms, Bandwidth723/770: Echo Spacing: 0.32 ms, Flip Angle:90, Matrix:192 × 192/180 × 180, no gap, IPAT = 2). For both sequences, 12 directions were obtained at each diffusion-weighting strength of b-250, 500, and 800 s/mm² (voxel: 1.3 × 1.3 × 2.2 mm) for 16 axial slices centered over the optic chiasm with oblique sagittal rotation to include the optic nerves, tracts, and as much of the optic radiations as possible. To match acquisition time for the rsDTI images, six averages were acquired for the ssDTI scan. RsDTI required 12 min 10 s to perform and ssDTI required 12 min and 19 s. At our institution, sedation for clinical MRI exams is routinely used for children from 3 months to 7 years of age. Exams were excluded if there was motion degradation as determined by a board certified neuroradiologist (CH, 10 years of experience).

B0 maps for ssDTI and rsDTI in all subjects were qualitatively evaluated by the board-certified neuroradiologist (CH) blinded to the DTI technique used based on a 5-point Likert scale. A score of 1 represents optic pathways completely obscured by susceptibility artifact to a score of 5, which represents no distortion. Two-tailed Wilcoxon signed rank test was used to assess for a significant difference between the two techniques.

Diffusion metrics (fractional anisotropy: FA, mean diffusivity: MD, axial diffusivity: AD, and radial diffusivity: RD) were computed and deterministic fiber tracking [8] were performed using DSI Studio (<http://dsi-studio.labsolver.org>). A seeding region was placed at both the right or left optic radiations, approximately 5 mm posterior to the optic chiasm, and a secondary inclusion region of interest (ROI) was placed on the optic chiasm (seeding: 10,000, angular threshold: 60°, step size: 0.6 mm, track minimum length 30 mm). All ROIs were placed on the FA maps. All ROIs were placed by a trained analyst (RD) in conjunction with a board-certified neuroradiologist (CH). For tumors involving the chiasm, tract, or radiations, ROIs were placed within the tumor at the expected epicenter of the native optic pathway (Fig. 1). To focus only on the effects of the ssDTI geometric distortion on the optic nerves, both tracts originating from the left and right optic radiations were merged and cut at

the narrowest coronal plane of the optic chiasm and posterior optic radiations were removed (Fig. 2). Scans with too much susceptibility distortion to result in any successful tract fibers were considered a zero for tract count, volume, and length.

Tract count, volume, and length along with diffusion metrics were compared. Two-factor mixed analysis of variance was used to accommodate for both within-group comparisons (between ssDTI and rsDTI within group patients) as well as between group comparisons (between tumor or visual symptom groups and healthy controls) using SPSS linear mixed model. Tract and diffusion metrics were normally distributed and tested with Shapiro-Wilk except for tract length ($p < 0.01$). Due to small sample sizes, multiple comparison corrections were not performed, and all data points were kept for statistical analysis. A two-tailed t test was used to assess for significant differences between the NF1 patients who had chemotherapy compared to NF1 patients without chemotherapy. Finally, observed power and effect size were reported as partial η^2 (IBM SPSS 24).

Results

Clinical characteristics

A total of 5 healthy children, 7 children with NF 1 without OG, and 12 children with NF1 with OG were imaged. Age range was 2 to 18 years of age (mean 8.9 years, 12 females). Eleven patients required sedation for the exam, and no exams were excluded due to motion. Of the patients with OG, 6 had visual symptoms (Table 1). A total of seven subjects had concurrent or a history of chemotherapy. Two subjects had concurrent chemotherapy with vincristine and carboplatin during the time of scan. Four subjects had 1.5–6 years of previous vincristine and carboplatin and one subject had a course of sunitinib malate 2 years prior to therapy for the treatment of a plexiform neurofibroma as part of an investigational clinical trial.

Qualitative Likert scale

Figure 3 shows the less susceptibility distortion on FA maps for rsDTI compared to ssDTI. One subject had no detectable optic pathway fibers bilaterally, two subjects had no left optic nerve, and one subject had no right optic nerve fibers detected on ssDTI. Qualitative evaluation using a Likert scale demonstrated a significantly greater mode and median for rsDTI (3, range 3 [2–5] compared to ssDTI (2, range 4 [1–5], $p < 0.001$), indicating that rsDTI had better subjective visualization of the optic pathway and less distortion.

RsDTI vs ssDTI—all subjects

In all subjects, rsDTI was able to delineate fibers for each optic nerve. For all subjects including healthy controls, rsDTI had significantly increased tract count, tract length, tract volume, and FA compared to ssDTI. Furthermore, rsDTI had significantly decreased MD, AD, and RD compared to ssDTI (Table 2).

RsDTI vs ssDTI—within groups

When comparing within-subject groups for HC, NF1, with OG and NF1 without tumor, rsDTI continued to produce significantly greater tract count, tract volume, and FA for the

NF1 subject groups. Significantly decreased MD and RD were seen for rsDTI vs ssDTI within the NF1 group without tumor and significantly decreased MD, AD, and RD for the NF1 group with tumor. However, tract count, length, and volume were not significantly different in HC between the two techniques (Table 3).

When comparing within-subject groups for HC, NF1 without visual symptoms, and NF1 with visual symptoms, significant increase in tract count and volume were noted in the NF1 with and without visual symptom groups between the two DTI techniques. FA was significantly increased in all groups between the two techniques. MD, AD, and RD were significantly decreased in rsDTI compared to ssDTI for the NF1 group without visual symptoms. Only RD was significantly decreased for rsDTI within the NF1 with visual symptom group. Again, tract count, length, and volume were not significantly different in HC between the two techniques (Table 4).

When comparing rsDTI and ssDTI within groups for NF1 with chemotherapy and NF1 without chemotherapy, there were similar results with significantly increased tract count, volumes, and FA for both groups and decreased MD, AD, and RD for the NF1 no chemotherapy group for rsDTI versus ssDTI (Table 5).

Between-group comparisons

Comparisons were performed between groups within the same technique to evaluate for differences based on the presence of NF1, tumor, visual symptoms, or chemotherapy. There was a significant decrease of MD, RD, and AD in the ssDTI technique between the NF1 with visual symptoms and NF1 without visual symptoms (Table 6). Similarly, NF1 patients with chemotherapy had significantly decreased measures of MD, AD, and RD compared to NF1 patients without chemotherapy only within the ssDTI technique (Table 7). No significant difference was seen across patient groups with the rsDTI technique (Appendix Tables 10, 11, 12, and 13).

Observed power and effect size

Finally, observed power and effect size were calculated for rsDTI vs ssDTI in all subjects and within patient groups. Adequate power (> 0.8) was noted for tract count, tract volume, FA, and RD for comparison of the techniques in all subjects and within groups (Tables 8 and 9). Comparison of different groups for the effect of NF1, tumor, visual symptoms, or chemotherapy did not have adequate power (Table 9).

Discussion

RsDTI vs ssDTI

In our study, we were able to demonstrate the superiority of rsDTI in qualitative and quantitative evaluation. RsDTI was able to produce significantly improved diffusion tensor data in terms of tract volume and count for the optic nerves particularly when challenged by the susceptibility artifact of the anatomy inherent within the anterior skull base. Tract count, length, and volume do not necessarily represent a 1:1 representation of the actual number of nerve fibers, nerve length, or thickness, which cannot be evaluated without sacrificing the

optic nerve. However, both techniques were processed in an identical manner, and the more robust technique with less susceptibility distortion can reasonably be expected to have a significantly higher result in these parameters, which we have demonstrated for rsDTI in both tract count and volume. rsDTI utilizes a multishot EPI technique, in which signal intensity acquisition is divided into multiple shots with interleaved and concatenated k-space trajectories. This requires a 2D navigator echo to correct for phase variations between shots which leads to increased scanning time but at the benefit of increased resolution and decreased susceptibility distortion [9, 10]. To control for scanning time, additional averages were added to ssDTI which would increase signal to noise as well as reduce distortion. Motion limitation of both scan types would be equally affected and did not invalidate any of the scans in our cohort.

FA, which is a representation of the magnitude of the diffusion of water molecules along a single axis, particularly along white matter tracts, is also commonly used in the literature as a quantitative MR parameter for a measure of tract integrity. When comparing two techniques, a higher FA would suggest a tract with less disruption, presumably by artifact in our experiment. Furthermore, FA was also significantly higher for rsDTI within the subject groups due to greater resolution and less susceptibility distortion for the small optic nerve as well as less volume averaging with the cerebral spinal fluid surrounding the prechiasmatic optic nerves. Similarly, with similar parallel imaging acceleration, our data supports the theoretical expectation of approximately a third of the distortion of rsDTI (0.32 ms) compared to ssDTI (0.94 ms) based on echo spacing.

Jeong et al. [11] recently reported using a multishot high-resolution EPI vs single shot EPI technique for tractography on the optic nerve in 15 healthy human volunteers. They found that multishot EPI had less qualitative distortion and less quantitative difference between right and left optic nerves and was more reproducible at a higher resolution when compared to single shot EPI. Comparatively, our study is the first to our knowledge to report findings on multishot EPI techniques between healthy volunteers and NF1 children with and without tumors. Our findings are similar in demonstrating the improvement for multishot EPI for delineating increases in tract volume and number compared to single shot EPI. However, there are significant differences in analysis. We used a tract-based analysis based on seeding from the optic tracts and chiasm, which would have less distortion than the prechiasmatic optic nerve due to the proximity of the bone and sinuses. Jeong et al. placed ROIs on the optic nerves of the mean diffusivity map which can be susceptible to distortion and may affect ROI accuracy.

There have been prior reports on the use of DTI in the optic pathway for NF1 patients; however, none of these have addressed the problem of susceptibility artifact affecting the quantification of parameters in the anterior pathway of the optic nerve and chiasm. In a mouse model genetically engineered to develop NF1 and OG, Hegedus et al. [12] demonstrated progressive decreased FA and increased RD from 3 weeks to 6 months as OG developed. No difference was demonstrated between these NF1 mice and wild-type mice before 3 weeks, the time frame before OG developed. It is important to note that in this mouse study, Hegedus et al. used a conventional spin echo technique instead of echo planar imaging to perform DTI, which would require long scanning times not practical for clinical

use but does not suffer from susceptibility artifacts. Furthermore, the technical comparison of mouse anatomy to human anatomy would also be difficult regarding susceptibility artifact at the skull base. In human subjects, Filippi et al. [13] and Nickerson et al. [14] in related studies on 9 NF1 patients and 44 and 70 controls, respectively, report quantitative data for optic nerve FA, MD, and ADC. They used conventional single shot EPI and marked small voxel ROIs for the optic nerves on T2-weighted anatomic images, with no comment about how the susceptibility artifact was overcome. Data from this voxel-based approach may be less reliable as using T1- or T2-weighted anatomic images for ROI placement would be less likely to translate appropriately to the distortion on EPI images from susceptibility. Again, we used a tract-based approach, which depends on mathematical analysis to generate tracts with less dependence on image registration [15].

Similarly, de Blank et al. [16] also used a tract-based approach and report that FA decrease is associated with visual acuity loss in NF1 patients versus NF1 patients without visual loss as controls. However, they found the significant FA decrease only in the optic radiations but not in the optic nerves. In their discussion, they write “Small white matter structures, such as optic nerves and tracts, can be difficult to isolate on DTI without partial voluming, and these pathways may be subject to susceptibility artifacts. The lack of a significant difference in FA of these structures may be attributable to the difficulty in measuring these anterior pathways accurately.” This emphasizes the importance of using a technique which is high resolution and limits the susceptibility artifact of the anterior skull base. While quantification of distal but connected tracts such as the optic radiations will likely produce a change, assessment of the fibers at or immediately adjacent to tumor development will likely produce the highest sensitivity in association with visual loss. This is similar to a study by Ellingson et al. [17], where DTI measures were performed on ten subjects with chronic spinal cord injury showing the greatest decrease in FA and greatest increase in diffusivity measures at or immediately adjacent to the level of injury compared to healthy controls. At levels more remote from the site of spinal cord injury, the differences in these measures were less pronounced, suggesting the greatest sensitivity of correlating with function lies near the site of injury.

Further implications from this study suggest that a DTI technique with increased resolution and less susceptibility artifact would be a better choice for studies where quantitative evaluation of the optic nerve can serve as a biomarker for visual function in very young children, and as a measure of improving health of the optic nerve with treatment.

Comparison between patient groups

Although we were able to demonstrate the technical superiority of rsDTI in delineating the optic nerves with adequate power, we were only able to find a significant decrease in mean, axial, and radial diffusivity in NF1 patients with visual symptoms and chemotherapy, compared to NF 1 patients without visual symptoms or chemotherapy. This contradicts the previous literature of increased mean and radial diffusivity associated with visual loss or pathology due to optic tumors [13, 14, 16, 18]. Furthermore, this significant decrease in diffusivity was only found on the conventional ssDTI scans and not the rsDTI technique. Although this result may be spurious due to the inadequate power of NF1 subjects measured

with and without visual symptoms, Ellingson et al. [17] also detected the finding of decreased diffusivity cranial to the site of spinal cord injury but not caudal. This has also been demonstrated in animal models and has been postulated to be related to chronic changes of axonal restructuring and widespread cord degeneration. Previous or concurrent chemotherapy also showed similar decreases in diffusivity; however, as the visual symptom and chemotherapy groups were nearly identical except for one subject, we cannot isolate the chemotherapy effect on the diffusivity parameter. De Blank et al. [19] were able to find a significant decrease in FA of the central white matter tracts of the brain in NF1 patients treated with vincristine and carboplatin compared to NF1 patients without prior treatment. Although we could expect FA to decrease in our patients with chemotherapy and visual symptoms compared to controls, we did not find a significant difference for the FA of the optic nerves in our study. Although we had enough power to demonstrate the technical superiority of rsDTI to ssDTI, we likely did not have enough power to demonstrate an effect of decreased optic nerve integrity as represented by the presence of visual symptoms. Another factor is the decision to calculate the bilateral optic nerves as merged tracts per patient instead of individually. This is due to the greater propensity of NF1 OG to involve the optic chiasm, which would theoretically affect quantitative parameters for both optic nerves. Accordingly, our study also showed most optic gliomas involving the chiasm, with only 2/6 with visual symptoms demonstrating unilateral optic nerve glioma on MRI.

Limitations

Our study had inadequate power to assess for differences between patient groups. Further study with larger power is needed to confirm quantifiable differences correlated to visual symptoms. While rsDTI represents an improvement for EPI-based techniques at limiting susceptibility artifact, we still noticed a small amount of distortion, particularly for older patients where the size of the sphenoid sinus allowed a greater amount of air near the anatomy of interest. A robust DTI technique with limited inherent susceptibility artifact such as spin echo techniques at clinically acceptable scan times may ultimately be a better alternative. Twelve-minute scan times for a single sequence is also limited in clinical usefulness. Newer technology using simultaneous multi-slice may decrease imaging time by greater than 50%, depending on the acceleration factor, but comes at the cost of slice signal leakage from aliasing [20].

Conclusion

High-resolution DTI with readout-segmented multi-shot EPI technique can better visualize the optic pathway, particularly the optic nerve and chiasm, which can be affected by susceptibility artifact. This is shown by a significant increase in FA, tract count, and volume with rsDTI versus ssDTI. This may allow more confident measurements of anisotropy and diffusivity in NF1 patients who develop OG with visual deficits and may serve as a marker for treatment initiation and follow-up.

Acknowledgments

Funding This study was funded by Chie-Schin Shih and an American Cancer Society Institutional Research Award (IRG-84-002-25).

Appendix 1

Table 10

Comparison between healthy controls and NF1 patients with and without optic pathway tumors for ssDTI scan type. Data reported as mean \pm standard error of mean

	Scan type	Tract count	Tract length	Tract volume	FA	MD	AD	RD
Healthy control	ssDTI	1182.8 \pm 145.9	6.8 \pm 1.5	686.8 \pm 178.7	0.29 \pm 0.02	1.92 \pm 0.13	2.42 \pm 0.13	1.68 \pm 0.12
HC vs NF_1 no tumor	p value	0.524	0.819	0.313	0.786	0.932	0.893	0.955
NF_1 + no tumor	ssDTI	849.9 \pm 291.9	6.3 \pm 1.2	476.0 \pm 133.7	0.30 \pm 0.01	1.91 \pm 0.07	2.39 \pm 0.09	1.67 \pm 0.07
HC vs NF_1 + tumor	p value	0.652	0.298	0.197	0.588	0.927	0.974	0.901
NF_1 + tumor	ssDTI	968.9 \pm 303.7	4.8 \pm 0.8	413.8 \pm 95.8	0.28 \pm 0.02	1.96 \pm 0.14	2.44 \pm 0.15	1.72 \pm 0.14
NF_1 + no tumor vs NF_1 + tumor	p value	0.778	0.372	0.820	0.354	0.837	0.841	0.836

Table 11

Comparison between healthy controls and NF1 patients with and without optic pathway tumors for rsDTI scan type. Data reported as mean \pm standard error of mean

	Scan type	Tract count	Tract length	Tract volume	FA	MD	AD	RD
Healthy control	rsDTI	1812.8 \pm 539.5	10.0 \pm 5.1	709.8 \pm 198.6	0.41 \pm 0.02	1.77 \pm 0.20	2.43 \pm 0.24	1.44 \pm 0.18
HC vs NF_1 no tumor	p value	0.512	0.441	0.539	0.380	0.326	0.279	0.369
NF_1 + no tumor	rsDTI	2204.5 \pm 322.3	7.8 \pm 1.6	942.3 \pm 153.0	0.38 \pm 0.02	1.52 \pm 0.10	2.09 \pm 0.13	1.24 \pm 0.08
HC vs NF_1 + tumor	p value	0.661	0.316	0.202	0.911	0.314	0.285	0.339
NF_1 + tumor	rsDTI	2061.6 \pm 313.7	7.1 \pm 1.0	1094.9 \pm 143.2	0.41 \pm 0.02	1.49 \pm 0.12	2.08 \pm 0.15	1.20 \pm 0.10
NF_1 + no tumor vs NF_1 + tumor	p value	0.741	0.855	0.480	0.325	0.929	0.882	0.967

Table 12

Comparison between healthy controls and NF1 patients with and without visual symptoms for rsDTI scan type. Data reported as mean \pm standard error of mean

	Scan type	Tract count	Tract length	Tract volume	FA	MD	AD	RD
Healthy control	rsDTI	1812.8 \pm 539.5	10.0 \pm 5.1	709.8 \pm 198.6	0.41 \pm 0.02	1.77 \pm 0.20	2.43 \pm 0.24	1.44 \pm 0.18

	Scan type	Tract count	Tract length	Tract volume	FA	MD	AD	RD
HC vs NF_1 + no visual	<i>p</i> value	0.377	0.304	0.323	0.547	0.448	0.403	0.487
NF_1 + no visual	rsDTI	2289.3 ± 265.0	7.2 ± 1.2	1015.5 ± 149.3	0.39 ± 0.02	1.58 ± 0.10	2.17 ± 0.13	1.28 ± 0.09
HC vs NF_1 + visual	<i>p</i> value	0.928	0.472	0.286	0.955	0.109	0.091	0.129
NF_1 + visual	rsDTI	1787.2 ± 421.1	7.7 ± 1.0	1088.0 ± 138.6	0.42 ± 0.03	1.37 ± 0.14	1.91 ± 0.17	1.10 ± 0.13
NF_1 + no visual vs NF_1 + visual	<i>p</i> value	0.264	0.781	0.814	0.448	0.228	0.216	0.243

Table 13

Comparison of rsDTI scans for NF_1 subjects with and without concurrent chemotherapy

	Scan type	Tract count	Tract length	Tract volume	FA	MD	AD	RD
NF_1 No Chemo	rsDTI	2234.3 ± 286.6	7.04 ± 1.3	1047.3 ± 161.3	0.40 ± 0.02	1.55 ± 0.11	2.15 ± 0.14	1.25 ± 0.09
NF_1 + Chemo	rsDTI	1937.4 ± 386.3	7.8 ± 0.85	1031.9 ± 129.7	0.41 ± 0.02	1.43 ± 0.13	2.00 ± 0.16	1.16 ± 0.12
<i>p</i> value		0.537	0.672	0.945	0.829	0.484	0.437	0.527

References

- Fisher MJ, Loguidice M, Gutmann DH, Listerick R, Ferner RE, Ullrich NJ, Packer RJ, Tabori U, Hoffman RO, Ardern-Holmes SL, Hummel TR, Hargrave DR, Bouffet E, Charrow J, Bilaniuk LT, Balcer LJ, Liu GT (2012) Visual outcomes in children with neurofibromatosis type 1-associated optic pathway glioma following chemotherapy: a multicenter retrospective analysis. *Neuro-Oncology* 14(6):790–797 [PubMed: 22474213]
- Kaufman LM, Doroftei O (2006) Optic glioma warranting treatment in children. *Eye(Lond)* 20(10):1149–1164 [PubMed: 17019413]
- Toledano H, Muhsinoglu O, Luckman J, Goldenberg-Cohen N, Michowiz S (2015) Acquired nystagmus as the initial presenting sign of chiasmal glioma in young children. *Eur J Paediatr Neurol* 19(6):694–700 [PubMed: 26190013]
- Schmitz B, Schaefer T, Krick CM, Reith W, Backens M, Ka'smann-Kellner B (2003) Configuration of the optic chiasm in humans with albinism as revealed by magnetic resonance imaging. *Invest Ophthalmol Vis Sci* 44(1):16–21 [PubMed: 12506050]
- Thiagalingam S, Flaherty M, Billson F, North K (2004) Neurofibromatosis type 1 and optic pathway gliomas: follow-up of 54 patients. *Ophthalmology* 111(3):568–577 [PubMed: 15019338]
- Zeid JL, Charrow J, Sandu M, Goldman S, Listerick R (2006) Orbital optic nerve gliomas in children with neurofibromatosis type 1. *JAAPOS* 10(6):534–539
- Zhao M, Liu Z, Sha Y, Wang S, Ye X, Pan Y, Wang S (2016) Readout-segmented echo-planar imaging in the evaluation of sinonasal lesions: a comprehensive comparison of image quality in single-shot echo-planar imaging. *Magn Reson Imaging* 34(2): 166–172 [PubMed: 26541548]
- Yeh FC, Verstynen TD, Wang Yet al. (2013) Deterministic diffusion fiber tracking improved by quantitative anisotropy. *PLoS One* 8(11):e80713 [PubMed: 24348913]
- Yamashita K, Yoshiura T, Hiwatashi A, Kamano H, Dashjamts T, Shibata S, Tamae A, Honda H (2011) Detection of middle ear cholesteatoma by diffusion-weighted MR imaging: multishot echo-

- planar imaging compared with single-shot echo-planar imaging. *AJNR Am J Neuroradiol* 32(10):1915–1918 [PubMed: 21778245]
10. Porter DA, Heidemann RM (2009) High resolution diffusion-weighted imaging using readout-segmented echo-planar imaging, parallel imaging and a two-dimensional navigator-based reacquisition. *Magn Reson Med* 62(2):468–475 [PubMed: 19449372]
 11. Jeong HK, Dewey BE, Hirtle JA et al. (2015) Improved diffusion tensor imaging of the optic nerve using multishot two-dimensional navigated acquisitions. *Magn Reson Med* 74(4):953–963 [PubMed: 25263603]
 12. Hegedus B, Hughes FW, Garbow JR, Gianino S, Banerjee D, Kim K, Ellisman MH, Brantley MA Jr, Gutmann DH (2009) Optic nerve dysfunction in a mouse model of neurofibromatosis-1 optic glioma. *J Neuropathol Exp Neurol* 68(5):542–551 [PubMed: 19525901]
 13. Filippi CG, Bos A, Nickerson JP, Salmela MB, Koski CJ, Cauley KA (2012) Magnetic resonance diffusion tensor imaging (MRDTI) of the optic nerve and optic radiations at 3T in children with neurofibromatosis type I (NF-1). *Pediatr Radiol* 42(2):168–174 [PubMed: 21858653]
 14. Nickerson JP, Salmela MB, Koski CJ, Andrews T, Filippi CG (2010) Diffusion tensor imaging of the pediatric optic nerve: intrinsic and extrinsic pathology compared to normal controls. *J Magn Reson Imaging* 32(1):76–81 [PubMed: 20578013]
 15. Van Hecke W, Leemans A, Emsell L (2016) DTI analysis methods: voxel-based analysis In: Van Hecke W, Emsell L, Sunaert S (eds) *Diffusion tensor imaging*. Springer, New York, pp 183–203
 16. de Blank PM, Berman JI, Liu GT et al. (2013) Fractional anisotropy of the optic radiations is associated with visual acuity loss in optic pathway gliomas of neurofibromatosis type 1. *Neuro-Oncology* 15(8):1088–1095 [PubMed: 23658320]
 17. Ellingson BM, Ulmer JL, Kurpad SN, Schmit BD (2008) Diffusion tensor MR imaging in chronic spinal cord injury. *AJNR Am J Neuroradiol* 29(10):1976–1982 [PubMed: 18719029]
 18. Ertan G, Zan E, Yousem DM, Ceritoglu C, Tekes A, Poretti A, Huisman TAGM (2014) Diffusion tensor imaging of neurofibromatosis bright objects in children with neurofibromatosis type 1. *Neuroradiol J* 27(5):616–626 [PubMed: 25260209]
 19. de Blank PM, Berman JI, Fisher MJ (2016) Systemic chemotherapy and white matter integrity in tracts associated with cognition among children with Neurofibromatosis type 1. *Pediatr Blood Cancer* 63(5):818–824 [PubMed: 26757156]
 20. Risk BB, Kociuba MC, Rowe DB (2018) Impacts of simultaneous multislice acquisition on sensitivity and specificity in fMRI. *Neuroimage* 172:538–553 [PubMed: 29408461]

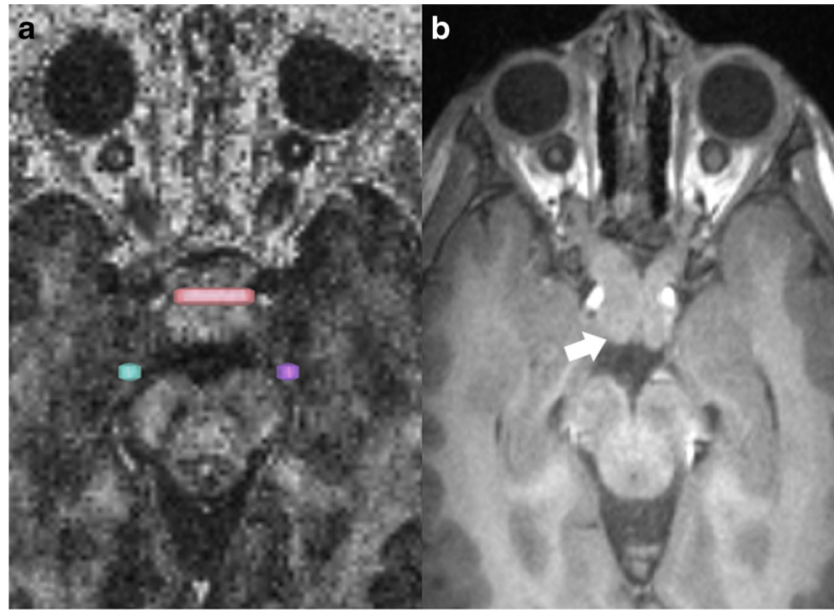


Fig. 1.
a Fractional anisotropy map shows ROIs placed in the bilateral optic tracts and within the expected epicenter of the chiasm involved by tumor **b** Axial T1-weighted anatomical image of the same patient showing the optic chiasm glioma (arrow)

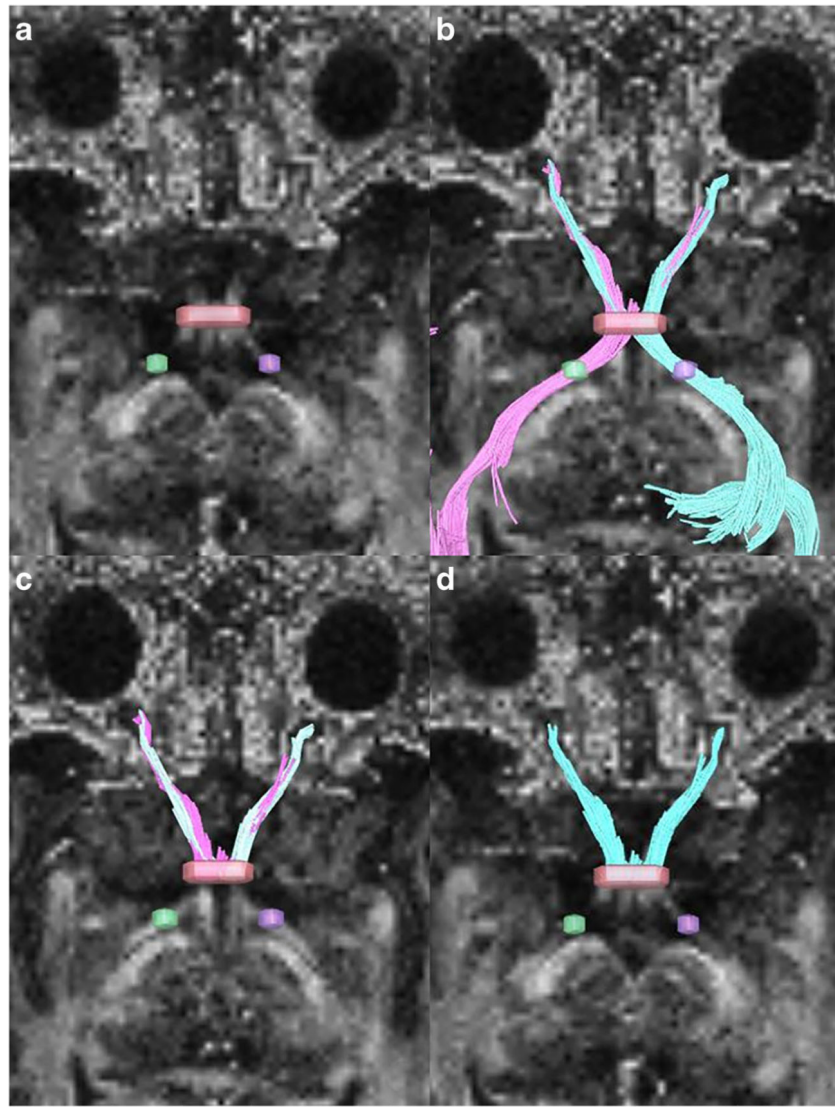


Fig. 2.
a Seeding placed on both optic tracts (purple and green) with region of interest on the chiasm (red). **b** Tracts generated from both left and right optic tract seeds and the chiasm. **c** Trimming of tracts behind the optic chiasm. **d** Merging of right and left tracts

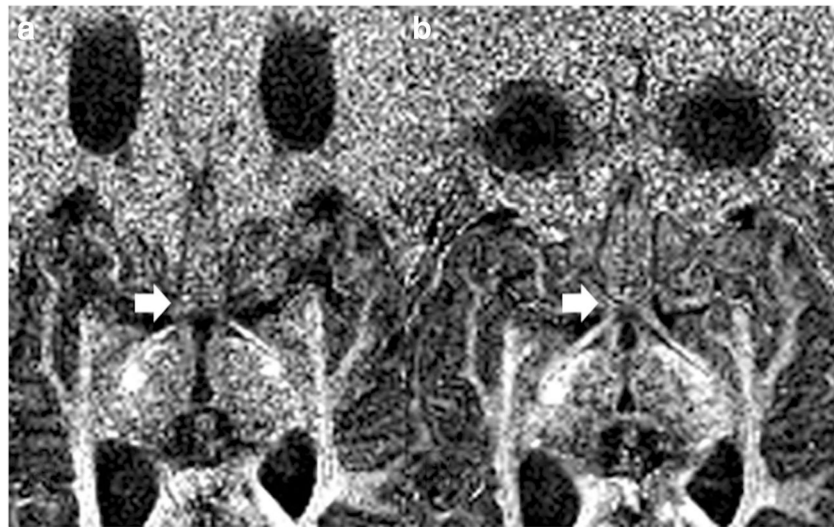


Fig. 3. ssDTI (**a**) vs rsDTI (**b**) on FA maps of subject 16. Note the improvement in susceptibility distortion of the optic chiasm and tracts (arrows) on the rsDTI image. There is also less distortion of the globes

Subject characteristics. All subjects with chemotherapy had vincristine and carboplatin, except for subject 14 who received sunitinib malate as part of a trial for plexiform neurofibromas

Table 1

Subject	Age at MRI (years)	NF1	Optic pathway tumor	Visual symptoms	Chemotherapy
1	9	Y	Y	Y-Left eye decreased vision	Y
2	7	Y	Y	N	N
3	13	Y	Y	N	N
4	14	Y	Y	Y-right vision loss	Y
5	3	Y	Y	Y-nystagmus and worsening vision	Y
6	7	Y	Y	N	N
7	3	Y	N	N	N
8	15	Y	Y	Y-Left eye decreased vision	Y
9	18	Y	Y	N	N
10	7	Y	Y	N	N
11	6	Y	N	N	N
12	11	Y	Y	Y-left eye decreased vision	Y
13	12	Y	Y	Y-decreased vision, nystagmus	Y
14	12	Y	N	N	Y
15	13	Y	N	N	N
16	12	Y	N	N	N
17	8	Y	N	N	N
18	7	Y	Y	N	N
19	2	Y	N	N	N
HC	5	N	N	N	N
HC	5	N	N	N	N
HC	4	N	N	N	N
HC	3	N	N	N	N
HC	17	N	N	N	N

Comparison of ssDTI and rsDTI for all subjects including healthy controls. Data reported as mean \pm standard error with significant p values from two-tailed paired t test are italicized

Table 2

Scan type	Tract count	Tract length	Tract volume	FA	MD	AD	RD
All subjects	978.8 \pm 172.9	5.6 \pm 0.6	488.8 \pm 72.0	0.29 \pm 0.01	1.94 \pm 0.07	2.42 \pm 0.08	1.69 \pm 0.07
rsDTI	2055.0 \pm 205.9	7.9 \pm 1.1	977.8 \pm 96.1	0.40 \pm 0.01	1.55 \pm 0.08	2.15 \pm 0.10	1.26 \pm 0.07
<i>p</i> value	<i>< 0.001</i>	<i>0.044</i>	<i>< 0.001</i>	<i>< 0.001</i>	<i>< 0.001</i>	<i>0.036</i>	<i>< 0.001</i>

Table 3
Comparison of scan types (ssDTI versus rsDTI) within patient groups. Data reported as mean \pm standard error of mean

	Scan type	Tract count	Tract length	Tract volume	FA	MD	AD	RD
Healthy control	ssDTI	1182.8 \pm 145.9	6.8 \pm 1.5	686.8 \pm 178.7	0.29 \pm 0.02	1.92 \pm 0.13	2.42 \pm 0.13	1.68 \pm 0.12
	rsDTI	1812.8 \pm 539.5	10.0 \pm 5.1	709.8 \pm 198.6	0.41 \pm 0.02*	1.77 \pm 0.20	2.43 \pm 0.24	1.44 \pm 0.18
	p value	0.219	0.219	0.639	< 0.001	0.339	0.960	0.135
NF_1 + no tumor	ssDTI	849.9 \pm 291.9	6.3 \pm 1.2	476.0 \pm 133.7	0.30 \pm 0.01	1.91 \pm 0.07	2.39 \pm 0.09	1.67 \pm 0.07
	rsDTI	2204.5 \pm 322.3*	7.8 \pm 1.6	942.3 \pm 153.0*	0.38 \pm 0.02*	1.52 \pm 0.10*	2.09 \pm 0.13	1.24 \pm 0.08*
	p value	0.004	0.575	0.009	0.002	0.019	0.115	0.006
NF_1 + tumor	ssDTI	968.9 \pm 303.7	4.8 \pm 0.8	413.8 \pm 95.8	0.28 \pm 0.02	1.96 \pm 0.14	2.44 \pm 0.15	1.72 \pm 0.14
	rsDTI	2061.6 \pm 313.7*	7.1 \pm 1.0	1094.9 \pm 143.2*	0.41 \pm 0.02*	1.49 \pm 0.12*	2.08 \pm 0.15*	1.20 \pm 0.10*
	p value	0.002	0.236	< 0.001	< 0.001	0.002	0.041	< 0.001

* Significant rsDTI vs. ssDTI within patient groups

Comparison of scan types (ssDTI versus rsDTI) in healthy controls and NF1 patients with and without visual symptoms. Data reported as mean \pm standard error of mean

Table 4

	Scan type	Tract count	Tract length	Tract volume	FA	MD	AD	RD
Healthy control	ssDTI	1182.8 \pm 145.9	6.8 \pm 1.5	686.6 \pm 178.7	0.29 \pm 0.02	1.92 \pm 0.13	2.42 \pm 0.13	1.68 \pm 0.12
	rsDTI	1812.8 \pm 539.5	10.0 \pm 5.1	709.8 \pm 198.6	0.41 \pm 0.02*	1.77 \pm 0.20	2.43 \pm 0.24	1.44 \pm 0.18
NF_1 + no visual	p value	0.221	0.222	0.652	0.001	0.344	0.974	0.131
	ssDTI	1073.3 \pm 291.4	5.1 \pm 0.8	449.5 \pm 88.2	0.27 \pm 0.01	2.09 \pm 0.10	2.57 \pm 0.11	1.85 \pm 0.10
NF_1 + Visual	rsDTI	2289.3 \pm 265.0*	7.2 \pm 1.2	1015.5 \pm 149.3*	0.39 \pm 0.02*	1.58 \pm 0.10*	2.17 \pm 0.13*	1.28 \pm 0.09*
	p value	0.001	0.356	< 0.001	< 0.001	< 0.001	0.016	< 0.001
NF_1 + Visual	ssDTI	603.8 \pm 235.5	5.8 \pm 1.3	408.8 \pm 158.9	0.31 \pm 0.02	1.64 \pm 0.09	2.11 \pm 0.11	1.40 \pm 0.09
	rsDTI	1787.2 \pm 421.1*	7.7 \pm 1.0	1088.0 \pm 138.6*	0.42 \pm 0.03*	1.37 \pm 0.14	1.91 \pm 0.17	1.10 \pm 0.13
	p value	0.015	0.390	0.001	0.001	0.099	0.291	0.047

* Significant rsDTI vs. ssDTI within patient groups

Table 5

Comparison of NF1 subjects with and without prior or concurrent chemotherapy. Data reported as mean \pm standard error

	Scan type	Tract count	Tract length	Tract volume	FA	MD	AD	RD
NF_1 No Chemo	ssDTI	1069.8 \pm 316.8	5.0 \pm 0.9	433.0 \pm 94.2	0.27 \pm 0.01	2.12 \pm 0.11	2.60 \pm 0.12	1.87 \pm 0.10
	rsDTI	2234.3 \pm 286.6*	7.04 \pm 1.3	1047.3 \pm 161.3*	0.40 \pm 0.02*	1.55 \pm 0.11*	2.15 \pm 0.14*	1.25 \pm 0.09*
<i>p</i> value		0.003	0.066	< 0.001	< 0.001	< 0.001	0.020	< 0.001
NF_1 + Chemo	ssDTI	676.9 \pm 212.0	5.72 \pm 1.1	443.1 \pm 138.6	0.31 \pm 0.02	1.66 \pm 0.08	2.14 \pm 0.09	1.43 \pm 0.08
	rsDTI	1937.4 \pm 386.3*	7.8 \pm 0.85	1031.9 \pm 129.7*	0.41 \pm 0.02*	1.43 \pm 0.13	2.00 \pm 0.16	1.16 \pm 0.12
<i>p</i> value		0.032	0.050	0.024	0.002	0.166	0.411	0.089

* Significant rsDTI vs. ssDTI within patient groups

Comparison between healthy controls and NF1 patients with and without visual symptoms for ssDTI scan type. Data reported as mean \pm standard error of mean

Table 6

	Scan type	Tract count	Tract length	Tract volume	FA	MD	AD	RD
Healthy control	ssDTI	1182.8 \pm 145.9	6.8 \pm 1.5	686.6 \pm 178.7	0.29 \pm 0.02	1.92 \pm 0.13	2.42 \pm 0.13	1.68 \pm 0.12
HC vs NF_1 + no visual	<i>p</i> value	0.810	0.426	0.267	0.467	0.371	0.435	0.344
NF_1 + no visual	ssDTI	1073.3 \pm 291.4	5.1 \pm 0.8	449.5 \pm 88.2	0.27 \pm 0.01	2.09 \pm 0.10	2.57 \pm 0.11	1.85 \pm 0.10
HC vs NF_1 + visual	<i>p</i> value	0.928	0.472	0.286	0.955	0.109	0.091	0.129
NF_1 + visual	ssDTI	603.8 \pm 235.5	5.8 \pm 1.3	408.8 \pm 158.9	0.31 \pm 0.02	1.64 \pm 0.09 [#]	2.11 \pm 0.11 [#]	1.40 \pm 0.09 [#]
NF_1 + no visual vs NF_1 + visual	<i>p</i> value	0.278	0.837	0.694	0.123	0.011	0.016	0.010

[#] Significant between NF1 patients without and with visual symptoms

Table 7

Comparison of ssDTI scans for NF_1 subjects with and without concurrent chemotherapy.

	Scan type	Tract count	Tract length	Tract volume	FA	MD	AD	RD
NF_1 No Chemo	ssDTI	1069.8 ± 316.8	5.0 ± 0.9	433.0 ± 94.2	0.27 ± 0.01	2.12 ± 0.11	2.60 ± 0.12	1.87 ± 0.10
NF_1 + Chemo	ssDTI	676.9 ± 212.0	5.72 ± 1.1	443.1 ± 138.6	0.31 ± 0.02	1.66 ± 0.08 [‡]	2.14 ± 0.09 [‡]	1.43 ± 0.08 [‡]
<i>p</i> value		0.393	0.651	0.951	0.072	0.009	0.012	0.008

[‡] Significant between NF1 patients with and without chemotherapy

Observed power analysis using $\alpha = 0.05$ and estimated effect size between ssDTI and rsDTI between all subjects

Table 8

	Tract count	Tract length	Tract volume	FA	MD	AD	RD
All subjects	0.976	0.368	0.971	0.999	0.937	0.567	0.990
Observed power	0.274	0.062	0.270	0.605	0.233	0.101	0.315
Partial Eta ²							

Observed power analysis using $\alpha = 0.05$ and estimated effect size within patient groups for scan type (ssDTI vs rsDTI) and between patient groups (healthy controls, NF_1 patients without tumors, and NF1 patients with tumors) for each scan type

Table 9

	Tract count	Tract length	Tract volume	FA	MD	AD	RD	
ssDTI vs rsDTI	Observed power	0.917	0.372	0.827	0.999	0.795	0.339	0.940
	Partial Eta ²	0.232	0.069	0.189	0.571	0.177	0.062	0.255
Healthy control, NF_1 ± tumor	Observed power	0.050	0.209	0.074	0.068	0.112	0.141	0.096
	Partial Eta ²	0.000	0.049	0.009	0.007	0.021	0.030	0.016